











Measurement of Platelet Aggregation in Ageing Samples and After in-Vitro Activation

Christian Klenk¹^a, David Elias Fresacher^{1,2}^b, Stefan Röhrl²^c, Dominik Heim¹^d,
Manuel Lengl²^e, Simon Schumann²^f, Martin Knopp¹^g, Klaus Diepold²^h,
Stefan Holdenrieder³ⁱ and Oliver Hayden¹^j

¹Heinz Nixdorf Chair for Biomedical Engineering, Technical University Munich, Arcisstr. 21, Munich, Germany

²Chair for Data Processing, Technical University Munich, Arcisstr. 21, Munich, Germany

³Institute for Laboratory Medicine, German Heart Centre Munich, Lazarettstr. 36, Munich, Germany

Keywords: Quantitative Phase Imaging, Microfluidics, Haematology, Machine Learning, Thrombocytes, Haemostasis, Digital Holographic Microscopy, Blood Cells, Flow Cytometry.

Abstract: Blood cell aggregates are gaining importance as a possible biomarker for various diseases. However, due to technical limitations of common analysers, mostly only interactions between leukocytes and platelets are measured directly as aggregates. Interactions between platelets are usually only measured indirectly after using an activation assay or by analysing surface proteins. Here, an imaging flow cytometer is used to measure and characterize platelet-aggregates directly in whole blood samples. Influences of sample ageing and in-vitro activation with adenosine diphosphate (ADP) was investigated for blood anticoagulated with either EDTA, citrate, heparin or hirudin. Here, the number of platelet-aggregates and their composition was measured. Blood anticoagulated with hirudin and EDTA showed a stable number of aggregates within a timeframe of 240 minutes. While no aggregate concentration changes were observed in EDTA blood after activation with ADP, a clear increase in aggregates was seen in hirudin, citrate and heparin blood. This effect is also observable when looking at the composition of the clots. However, after an initial spike a large number of aggregates disintegrate within a time frame of nine minutes. This effect is particularly prominent for large aggregates containing six or more platelets.


1 INTRODUCTION


The analysis of processes in haemostasis is a crucial field for medical diagnostics and the monitoring of interventions. By understanding the mechanisms behind haemostasis, specific dysfunctions can be detected and traced back to possible causes.


Haemostasis describes the process of regulating the formation of blood clots. This can result in the development of blood clots, to limit the extent of bleedings. In the opposite scenario, excessive thrombus


formation must be counteracted to prevent vascular occlusion. An important role in these processes involves blood platelets (thrombocytes), which are usually found as single cells and in an inactivated discoid shape. External factors can lead to an activation of platelets, which leads to a change in their morphology. This process triggers a number of reactions resulting in the formation of platelet-aggregates, in other words the cohesion of the platelets by fibrinogen (Kamath et al., 2001). If these cell clusters are not stabilised by fibrin strands, this usually results in unstable aggregates, which in turn often disintegrate within a few minutes (Michelson et al., 2001).


Various diseases can influence haemostasis in such a way that the formation of blood clots is either increased or inhibited. Prominent examples are the hyperactivity of platelets in blood of patients suffering from COVID-19 (Rampotas and Pavord, 2021) and cardiovascular diseases (Allen et al., 2019) as well as a reduced haemostasis in haemophilia (Riedl et al., 2017). In addition, the observation and targeted alteration of blood coagulation through drug


^a <https://orcid.org/0000-0002-4664-8107>


^b <https://orcid.org/0000-0002-7650-8033>


^c <https://orcid.org/0000-0001-6277-3816>


^d <https://orcid.org/0000-0001-8463-1544>


^e <https://orcid.org/0000-0001-8763-6201>

^f <https://orcid.org/0000-0002-7074-473X>

^g <https://orcid.org/0000-0002-1136-2950>

^h <https://orcid.org/0000-0003-0439-7511>

ⁱ <https://orcid.org/0000-0001-9210-7064>

^j <https://orcid.org/0000-0002-2678-8663>

interventions also play a major role in the treatment of patients. Thus, anticoagulant therapies are used to specifically inhibit blood coagulation in patients with various clinical conditions in order to counteract complications such as the formation of a thrombus (Lazaridis et al., 2021; Lazo-Langner et al., 2007). Nevertheless, it must be noted that an excessive administration of these pharmaceuticals can lead to increased bleeding events (Çankaya et al., 2021). For this reason, actions must be considered carefully and regularly controlled for every patient. A balance in the treatment with anticoagulants between the risks of thrombosis and bleeding can only be achieved with an in-depth knowledge of the patients state of health (Al-Samkari and Connors, 2019).

As a diagnostic tool of choice, coagulation is usually determined indirectly with the help of *in-vitro* analysers. Those devices determine dynamics in coagulation with the help of so-called activation assays. Here, an activating substance is added to the blood sample, which starts the process of blood clotting. The time and dynamics are measured until a certain sample volume is partially or completely clumped. The underlying technology for measuring this kind of assays can be determined both mechanically (Whiting and DiNardo, 2014) and by impedance measurement (Sibbing et al., 2008). Both methods have a wide range of possible applications but have the disadvantage that large sample volumes are usually required, and partial aspects of coagulation can only be measured after the use of an activation assay. The direct measurement of blood cell aggregates is an alternative approach, which generally does not suffer from these disadvantages. Aggregates can be measured using many different methods. One prominent example is the use of a so-called blood smear analysis (Rampotas and Pavord, 2021). Here, the cells are presented on a slide, stained and examined under a microscope. This method provides a high contrast, but requires trained personnel, time-consuming sample preparation steps and measures only a statistically small number of cells. Fluorescent flow cytometry combines fluorescent staining of blood cells with a microfluidic system and an optical readout (Michelson et al., 2001). This results in a rapid image acquisition and therefore in high numbers of measured cells in a short time frame. The highly specific binding of the fluorescent dye labelled antibodies allows accurate cell identification (Herzenberg et al., 2000). However, a major disadvantage is the low spatial resolution and the cost and time intensive staining. Especially the low spatial resolution makes a detection of small platelet-aggregates difficult.

Here, we present a method that combines the high

spatial resolution of an imaging method like the blood smear analysis with the level of automation in fluorescent flow cytometry by combining a quantitative phase contrast microscope with a microfluidic system and an adapted image analysis. This not only allows the measurement of aggregates in high throughput and without staining, but also allows a quantitative characterisation of their single components. In the work presented here, the method is applied for two purposes. First, to measure the influence of the ageing of blood samples on platelets aggregates (*P-aggregates*) while storing them in different blood collection tubes. And second, to measure dynamics in *P-aggregate* formation and decay when using a commonly used activation assay.

2 MATERIAL AND METHODS

The applied protocols and the methodology of the image-based flow cytometer used for the analysis of dynamics in cell aggregation are described in this section in more detail. The presented flow cytometer is composed of a digital holographic microscope (DHM), a microfluidic channel and a customized image analysis (see Figure 1). Previous to this work, this technique was already utilized to analyse changes in leukocyte morphology due to sample preparation (Klenk et al., 2019) and to distinguish between different types of leukaemia (Ugele et al., 2018).

2.1 Digital Holographic Microscopy

For the recording of the image data a transmission digital holographic microscope (Ovizio Imaging System) was used. Interferograms on the GS3-U3-32S4M camera (Teledyne FLIR LLC) are generated by off-axis holography combined with a double shearing interferometric approach. A 528 nm SLED (Osram) along with a Koehler illumination unit serves as a light source. Light passes through the sample towards the objective (CFI LWD, Nikon). The objective has a 40x magnification and a numeric aperture of 0.55 providing moderate resolution in both axial and lateral direction. A grating is used to generate diffraction maxima, which together with a spatial filter are essential for the in-line approach. Interference of the single beams is generated on the camera with a specific phase angle between them (off-axis) and results in the creation of an interferogram. Images are generated with a frame rate of 105 frames per second at an exposure time of 5 μ s using the Software Os-One Version 5.12.12 (Ovizio Imaging Systems). Each image contains on average 5 - 20 cells, resulting in

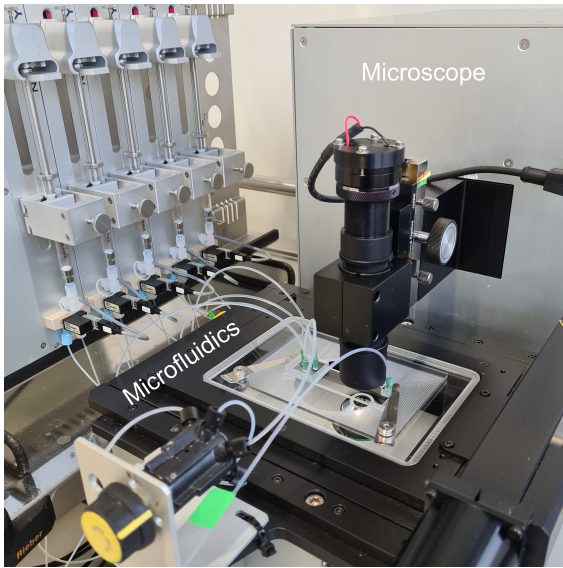


Figure 1: Hardware components of the optical flow cytometer containing a digital holographic microscope, a microfluidic channel and a syringe pump system.

525 - 2100 cells per second. This leads to approximately 50,000 measured blood cells per capture.

2.2 Microfluidics

A microfluidic system was implemented to achieve a high throughput of samples with a precise blood cell alignment in a sub monolayer. For this, a polymethylmethacrylate (PMMA) channel with a width of 500 μm , a height of 50 μm and a length of 5000 μm was used. Viscoelastic and hydrodynamic focussing methods were combined to ensure a high precision. To enable viscoelastic focussing, a portion of the polymer polyethylene oxide (PEO) was added to the measurement solution. Hydrodynamic focussing was implemented, using four sheath flows surrounding the sample from bottom, top and both sides. Additionally to the horizontal focussing this also allows a vertical alignment. The total flow rate was fixed to 1.6 $\mu\text{l/s}$ resulting in a flow velocity of 6.4 cm/s and a Reynolds number in a single digit range ($\text{Re} \approx 6$). Due to this low flow Reynolds number, experiments were carried out in the laminar flow regime.

2.3 Image Analysis

The analysis of the quantitative phase images was done in three distinct steps: preprocessing of the images, Mask R-CNN based segmentation, and analysis of detected objects.

- Preprocessing of the data included a background subtraction, cell detection, masking and normal-

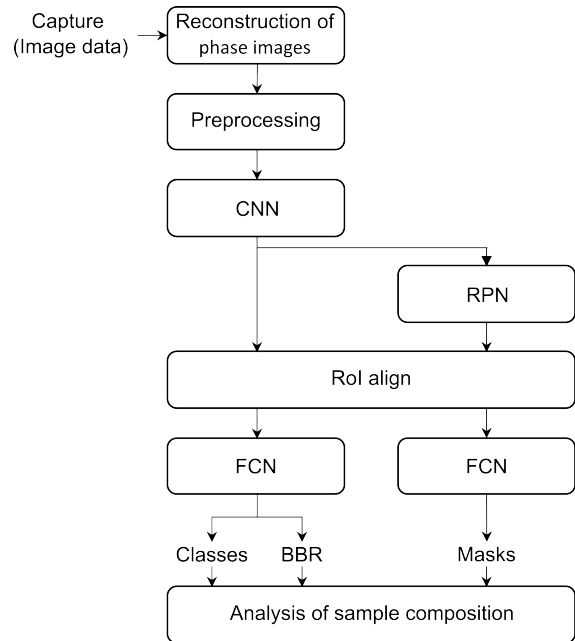


Figure 2: Block diagram of image analysis processes needed to get from the raw holographic images towards interpretable data.

ization. Background subtraction is needed to eliminate background noise due to channel walls and other phase influencing elements. By using threshold segmentation, binary images of the single elements were obtained. Contours of objects were extracted based on the thresholding results and the algorithm of Suzuki et al. (Suzuki et al., 1985). By choosing a suitable size filter on the contours of detected objects, background artefacts from measurement media or debris could be removed. As a final preprocessing step, normalisation steps were carried out which are serving two purposes. First, limiting the value range of the phase images and then normalizing them by a min-max normalisation to transform the image values into the range 0-1 which is suitable for neural networks.

- As a second level of segmentation a Mask R-CNN (He et al., 2017) approach was used for both a refinement of the segmentation contour and an instance segmentation of cell aggregates. Mask R-CNN performed both object detection and object mask computation at the same time and is based on the Faster R-CNN (Ren et al., 2015). This region-based convolutional neural network (CNN) operates in four stages. First, a CNN provides a convolutional feature map based on the input patches. Secondly, a region proposal network (RPN) provides regions of interest (RoI) by sliding a small network over the convolutional fea-

ture map. Then, a RoI align layer utilizes bi-linear interpolation to provide feature maps with the same size as the RoI. These are used in the fourth stage for classification and bounding box regression (BBR). In parallel, a small fully convolutional network (FCN) was applied to each RoI to predict the individual object masks at pixel resolution. For the analysis of aggregates in this work, a ResNet50 (He et al., 2016) was used as a convolutional network. For training, two datasets were used. One with single defined blood cells as well as a dataset with synthetically created aggregates. These were made by composing several single cell pictures together. Blood cells were classified in three different classes: red blood cells (erythrocytes), white blood cells (leukocytes) and platelets (thrombocytes). The network was trained on a total of 200,000 cell patches.

- Analysis of detected objects is the last step of the imaging analysis pipeline. Based on the segmentation and classification results, image patches are categorized as single cells or cell aggregates. This allows an analysis of the number of cells forming an aggregate and how this clot is structured. An example of a single platelet and platelet-aggregates with the corresponding results of the segmentation and classification is shown in Figure 3. Here, the highlighted green lines represent the borders of the segmentation. Green in this case represents a classified platelet.

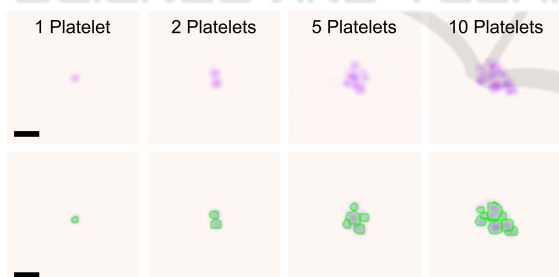


Figure 3: Example images showing single platelets and platelet-aggregates of different sizes. The top row shows the quantitative phase contrast images in false colour. The bottom row shows the same cells, with applied segmentation and classification by the image analysis algorithm. The highlighted edges represent the edges of the segmentation, with the colour illustrating the classification. Green in this case represents platelets. The scale bars correspond to 5 μ m.

2.4 Sample Preparation

Two different protocols were used for the experiments presented in this work. One for measuring the ageing of blood samples and the other for *in-vitro* activation of blood cells. In both cases, dilution was

performed by mixing the sample with a measurement solution containing 99.95 % phosphate buffered saline (PBS) and 0.05 % polyethylene oxide (PEO, molecular weight MW = 4×10^6 Da, Sigma Aldrich)

Table 1: Overview of the used anticoagulants and their concentrations specified by the supplier.

Name	Anticoagulant	Concentration
Citrate	Trisodium citrate	0.129 mmol/ml
EDTA	K3 Ethylenediamine-tetraacetic acid	1.6 mg/ml
Heparin	Lithium heparin	16 IU/ml
Hirudin	Hirudin	525 ATU Hirudin / ml

2.4.1 Ageing Experiment

Blood from a total of four independent donors ¹ was collected in the blood collection tubes mentioned in Table 1. Directly before the measurement, blood was diluted 1:100 in the measurement solution to reduce cell density.

2.4.2 In-vitro Activation Experiment

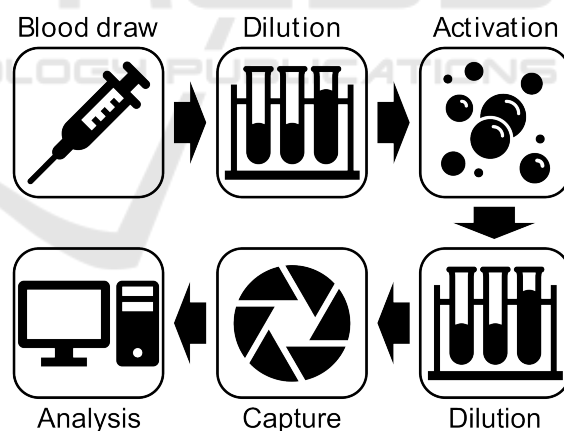


Figure 4: Schematic of sample preparation steps for the activation protocol.

For the *in-vitro* activation experiment, blood of three independent donors was drawn and collected in the same blood collection tubes mentioned in Table 1. After a subsequent dilution step (1:2 with PBS) and mixing for three minutes at 37°C, adenosine diphos-

¹All human samples were collected with informed consent and procedures approved by application 620/21 S-KK of the ethic committee of the Technical University Hospital of Munich

phate (ADP) with a final concentration of 0.33 μM , 1.61 μM or 6.45 μM was added as an activator. This step was followed by an additional dilution step (1:50 with measurement solution). Platelet-aggregates were measured continuously for twelve minutes. Since there were three to four minutes between each measurement, a total number of four measurements were carried out. Note, that the first measurement was performed shortly before the activation with ADP and that the first three preanalytical steps (see top row of Figure 4) are adapted from existing activation protocols to allow for comparability of results (Sibbing et al., 2008).

3 RESULTS

The findings of this study focus on the influence of sample ageing on aggregates as well as the change in blood after *in-vitro* activation by ADP. The measured target variables include the number and composition of *P-aggregates*. The number of *P-aggregates* is always given percentage to the total amount of platelets in the blood sample. The composition is described by the amount of the involved platelets. For this, the total of all *P-aggregates* is always normalized to 100 %.

3.1 Effect of Sample Ageing on Measured P-Aggregates

Blood of all donors was anticoagulated in citrate, EDTA, heparin and hirudin tubes. The storage and measurement of the sample was then performed at room temperature over a period of two hours. Figure 5a shows such a progression for one exemplary donor. After 0, 30, 60, 120 and 240 minutes, the *P-aggregates* were measured. The different anticoagulants are shown in different colours with citrate, EDTA, heparin and hirudin represented in black, blue, orange and green, respectively. All measurements within the 240 minutes of EDTA, citrate and hirudin range between 0.5 - 3 % of *P-aggregates*. For donor 1, there are only two outliers, namely in the heparin tube after 30 min (5.71 %) and 60 min (8.94 %). A similar picture can be seen when observing Figure 5b. Here, the aggregates of the ageing measurement are compared with the respective 0 min measurement for all patients and the difference is plotted on the Y-axis. Each point represents one measurement. In addition, the normal distribution fitted over all points was displayed. For EDTA and hirudin blood, an expected distribution around the origin can be observed. As for donor 1, heparin shows an increased aggregation compared to the zero measurement. Citrate, on the

other hand, shows a reduced aggregate number over time.

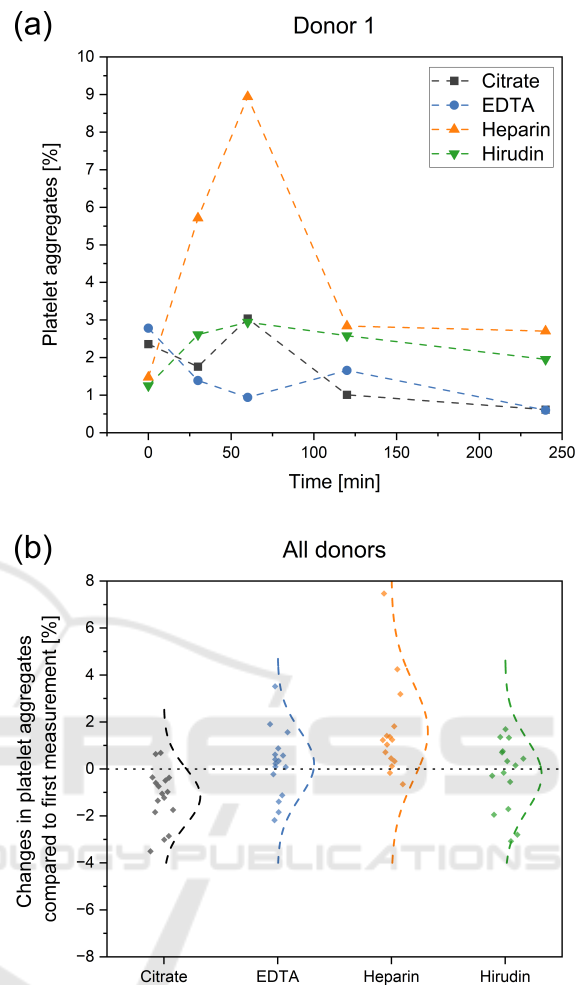


Figure 5: Ageing effects on the measured number of platelet-aggregates in different blood collection tubes. (a) Analysis of platelet-aggregate behaviour for different anticoagulants over a period of 240 minutes for one donor. (b) Difference in platelet-aggregate for all donors of the 30-, 60-, 120- and 240-minute measurement compared to their respective 0-minutes reference.

3.2 In-vitro Activation of Thrombocytes

In this section, the effects of activation assays on *P-aggregates* are investigated. For this, the ADP concentration was varied and different anticoagulants were used. The *in-vitro* activation protocol presented in chapter 2.4.2 was applied.

3.2.1 Impact of ADP Concentration

In a first step, the concentration of the added ADP for activation was varied to test whether this has an

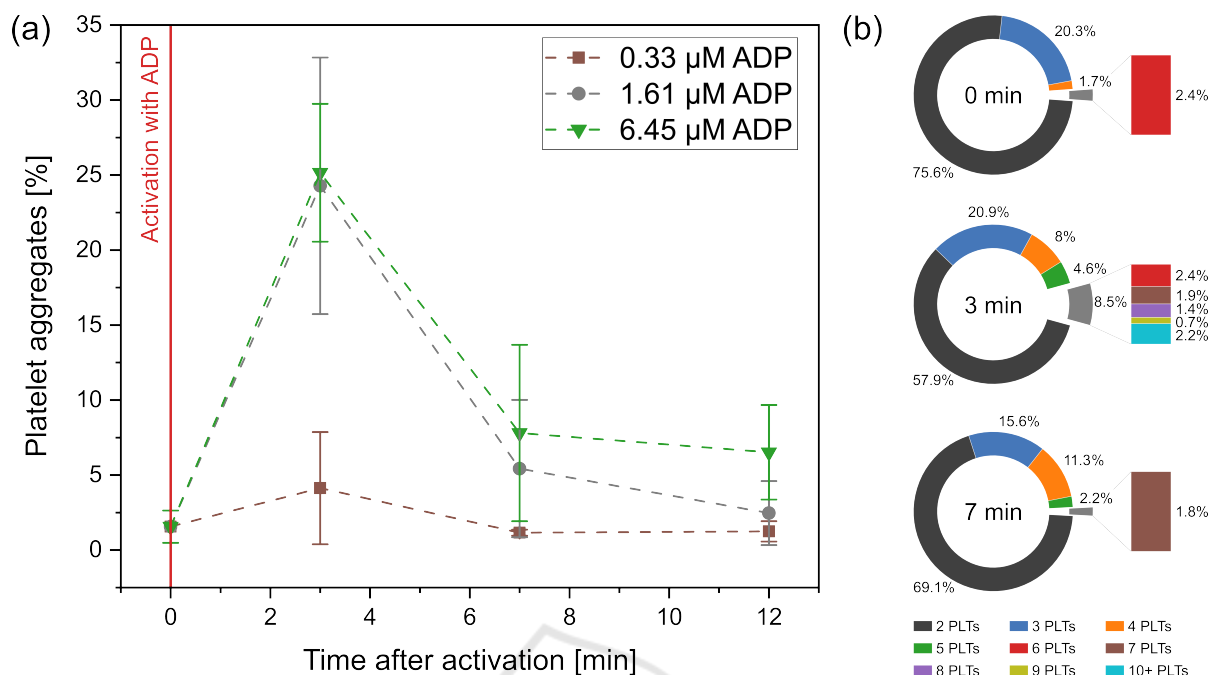


Figure 6: Change in the number (a) and composition (b) of platelet-aggregates over time after activation with different concentrations of ADP. In all three cases, blood was collected in a hirudin blood collection tube. For the characterization of the *P-aggregate* composition (b) all results are presented for the 6.45 μM experiment.

impact on the measured number and composition of *P-aggregates*. For this purpose, the starting concentration of ADP with 6.45 μM was diluted to 1.61 μM and 0.33 μM and added to hirudin blood samples. Measurements were taken shortly before activation (0 min) and after activation (3, 7 and 12 min). As shown in Figure 6a, the activation step results in an increase in aggregates after three minutes for all ADP concentrations. However, at 0.33 μM (brown squares) the value only slightly increases from 1.56 % to 4.13 %, whereas at 1.61 μM (gray circles) and 6.45 μM (green triangles) the values increase significantly more (to 24.28 % and 25.15 %). After reaching this maximum value of aggregation at three minutes, in all three cases the values decrease over time. A similar course can also be observed for the aggregate composition. Figure 6b shows the size distribution of the aggregates for the case of activation with 6.45 μM ADP. For the first measurement, most of the aggregates consist of two or three platelets. Only 4.1 % of the aggregates consist of more than three platelets. Immediately after activation, this proportion increases to 21.1 %. Particularly noteworthy is, clots with 10 or more platelets account for 2.2 % of all aggregates. For the seven-minute measurement not only a large share of aggregates disintegrated but especially the majority of large aggregates. At this point, aggregates with 10 or more platelets could no longer be observed.

3.2.2 Impact of Used Anticoagulants

The choice of anticoagulant influences the *in-vitro* activatability of blood cells. Thus, they intervene at different points in the coagulation cascade, preventing uncontrolled formation of large amounts of blood clots. To test whether these differences can also be observed when measuring *P-aggregates*, differently anticoagulated blood was activated with a total concentration of 6.45 μM ADP each. Figure 7 shows the difference between the single measurement points and their associated zero measurement before activation. Thus, differences due to activation can be observed directly for each point in time. When looking at the numbers of the EDTA measurement (blue circles) no significant increase in *P-aggregates* after activation can be observed. For all three measurement points the increase ranges between 0.16 % and 0.66 %. In contrast to this, a sharp increase can be observed for blood samples with citrate (black squares), heparin (orange triangles) and hirudin (green triangles). Directly after activation, the three values of the anticoagulants lie close to each other with values ranges from 21.68 % to 23.59 %. This rise is then followed by a drop at the time points 7 min and 12 min, whereby this decrease is lower for heparinized blood than for the other two anticoagulants.

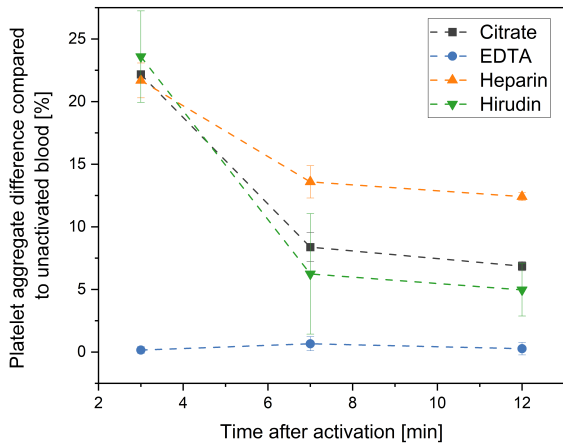


Figure 7: Influence of *in-vitro* activation on measured *P-aggregates* in blood samples with different anticoagulants. Shown is the difference in platelet-aggregate for all donors 3-, 7- and 12-minutes after activation compared to their respective 0-minutes value.

3.2.3 Decay of P-Aggregates by Size over Time

As shown in the previous chapters, *P-aggregates* tend to decay after an initial formation in the *in-vitro* activation experiments. The dynamics of this process are visible for citrate, heparin and hirudin as anticoagulant. In Figure 8, this decay was examined in term of the size of the decaying aggregates. For this purpose, all citrate, heparin and hirudin measurements were pooled. Aggregates were analysed at 3 and 12 minutes, by this the number of disintegrating clots within these nine minutes was determined. For this analysis aggregates were considered from a size of two platelets up to a size of ten platelets. Within the nine minutes of analysis, the majority of *P-aggregates* decayed. This effect could especially be observed in larger aggregate structures. While the number of remaining clots with two, three, four or five platelets were still between 41.03 % and 45.59 %, large aggregates tend to decay faster. In clots of six to nine platelets a nearly linear increase from 77.40 % to 100 % disintegrated *P-aggregates* could be seen. A slight decrease is then observed for structures with 10 PLTs (95.58 %), which might be due to the small amount of such large structures after 12 minutes and the associated measurement inaccuracy.

4 DISCUSSION

As shown in Figure 5 and 6, a stable measurement of blood was achieved. Measured aggregate values directly after blood draw laid between 0.50 % and 3.00 %, which is in a similar range as published

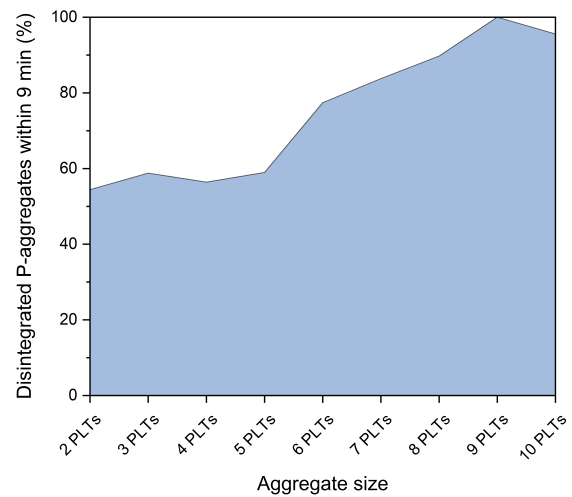


Figure 8: In depth analysis of *P-aggregate* decay by size between minute 3 and 12 of the activation experiments. For this purpose all measurements of citrate, heparin and hirudin were pooled and then analysed together.

data. Leytin et al. analysed the number of activated platelets by measuring P-selectin, a protein which is presented on the surface of the thrombocytes when activated (Leytin et al., 2000). Here, an amount of 1.02 ± 0.49 % of activated platelets could be observed for healthy blood samples. The slight difference in range to the here presented data could be explained by the use of different analysing techniques and the measurement of different biomarkers. Although the number of activated platelets and *P-aggregates* are directly related, it does not allow direct comparability of the values.

For samples without ageing effect, the measurements for EDTA and hirudin showed a normal distribution around the respective zero measurement (Figure 5b). The measured *P-aggregate* values tended to vary between ± 2 % during the two hours of monitoring, allowing stable measurement conditions. For heparinised blood on the other hand, an increased aggregate formation due to ageing effects could be observed. Since this is mostly observed shortly after blood collection (Figure 5a), thus after 30 and 60 min, these effects could be due to the blood collection and subsequent lower anticoagulation with heparin. For citrate blood a decrease of values over time, hence a disintegration of aggregates could be observed. Both effects, for citrate and heparin, show a clear trend for the four measured blood samples, but need to be validated by a higher sample collective in the future.

In addition to measuring ageing effects, the method was also applied to measure highly dynamic processes in the formation and decay of blood cell aggregates. Figure 6 - 8 show the rate of this dynamics. Depending on the anticoagulant, between 42.79 % -

79.98 % of all *P-aggregates* disintegrated within nine minutes. Michelson et al. performed a comparable study in-vivo. Here, they activated baboon platelet concentrates, infused it into the animals and measured the number of leukocyte-platelet-aggregates in the blood stream. For monocyte-platelet-aggregates approximately 72.73 % disintegrated within a time frame of ten minutes (Michelson et al., 2001). Although this experimental protocol and the measured aggregates cannot be compared directly to the *P-aggregates*, it still shows a similar physiological dynamic. The fast changes in values underline the need of a measurement technique which is not dependent on time consuming sample preparation steps or long acquisition times. Increased aggregate values can still be detected several minutes after activation, but on a reduced scale. Furthermore, it cannot be ruled out that the sample is activated due to sample preparation and handling (Ramstack et al., 1979; Jesty et al., 2003).

When observing *P-aggregate* formation, results in Figure 7 suggest that there was a difference in activation of blood, depending on the used anticoagulant. There were anticoagulants that allowed an *in-vitro* activation of blood with ADP, namely citrate, heparin and hirudin, and then there was EDTA, that prevented any activation. These results are in line with findings, showing that EDTA prevents an interaction between fibrinogen and the exposed receptors on the platelet membranes resulting in strongly inhibited formation of aggregates (Peerschke and Zucker, 1981). Citrate, heparin and hirudin on the other hand are commonly used for *in-vitro* activation assays and allow a subsequent blood coagulation (Wallén et al., 1997). Besides the chosen anticoagulant also the amount of added ADP had an impact on platelet activation. Thus, only a marginal increase in aggregates could be registered after activation with 0.33 μM ADP. The effects were significantly higher for 1.61 μM and 6.45 μM with only a small difference between these two concentrations. This suggests that saturation is reached and further concentration increase does not lead to a significant increase in *P-aggregates*.

Lastly, when looking at the composition of the *P-aggregates* it can be seen, that after activating blood with ADP not only the number of aggregates but also the number of the involved platelets changes. While the aggregates for the measurements before activation (Figure 6) mostly consisted of two platelets, the number of larger aggregates changed considerably after activation. The ADP promoted cohesion of platelets by fibrinogen, thus supports not only the formation of small but also large blood clots. When observing their decay (Figure 8), it can be seen that the proportion of large aggregates with more than six platelets

tended to dissolve faster than smaller aggregates. This effect may be explained by a homogeneous disintegration of all aggregates but a decay of big clots into smaller ones. Thus, nine minutes after activation, almost no aggregates with nine or more platelets could be recorded.

5 CONCLUSION

The work presented here, shows a method that is capable of high throughput measurement of *P-aggregates* without any staining or other lengthy sample preparations. Through combination of quantitative phase microscopy, microfluidics and image analysis a quantitative and qualitative analysis of these aggregates was achieved. This was done in such a way that even fast dynamics in aggregation formation and decay could be observed. When looking at the analysed anticoagulants, two reagents show promising results for long time storage of blood, regarding the measured *P-aggregates*. EDTA and hirudin fulfil this goal, whereby only the latter allows an *in-vitro* activation. The application of the presented method for ageing and activation measurements is a first step to characterise the measurement system as well as the biomarker. The long-term goal, however, is to measure increased platelet activity in blood of patients with various diseases. An increased platelet activity was already observed for patients with COVID-19, cancer and cardiovascular diseases. Although further studies are needed to validate the biomarker in these medical fields, the presented method could be a promising tool to reach this goal.

REFERENCES

- Al-Samkari, H. and Connors, J. M. (2019). Managing the competing risks of thrombosis, bleeding, and anticoagulation in patients with malignancy. *Hematology 2014, the American Society of Hematology Education Program Book*, 2019(1):71–79.
- Allen, N., Barrett, T. J., Guo, Y., Nardi, M., Ramkhelawon, B., Rockman, C. B., Hochman, J. S., and Berger, J. S. (2019). Circulating monocyte-platelet aggregates are a robust marker of platelet activity in cardiovascular disease. *Atherosclerosis*, 282:11–18.
- Çankaya, B. Y., Alper, F., Karaman, A., and Akgün, M. (2021). Hemorrhagic lesions associated with anticoagulant therapy: a pictorial review. *Journal of Thrombosis and Thrombolysis*, 51(4):1067–1077.
- He, K., Gkioxari, G., Dollár, P., and Girshick, R. (2017). Mask r-cnn. In *Proceedings of the IEEE international conference on computer vision*, pages 2961–2969.

- He, K., Zhang, X., Ren, S., and Sun, J. (2016). Deep residual learning for image recognition. In *Proceedings of the IEEE conference on computer vision and pattern recognition*, pages 770–778.
- Herzenberg, L. A., De Rosa, S. C., and Herzenberg, L. A. (2000). Monoclonal antibodies and the facts: complementary tools for immunobiology and medicine. *Immunology today*, 21(8):383–390.
- Jesty, J., Yin, W., Perrotta, P., and Bluestein, D. (2003). Platelet activation in a circulating flow loop: combined effects of shear stress and exposure time. *Platelets*, 14(3):143–149.
- Kamath, S., Blann, A., and Lip, G. (2001). Platelet activation: assessment and quantification. *European heart journal*, 22(17):1561–1571.
- Klenk, C., Heim, D., Ugele, M., and Hayden, O. (2019). Impact of sample preparation on holographic imaging of leukocytes. *Optical Engineering*, 59(10):102403.
- Lazaridis, D., Leung, S., Kohler, L., Smith, C. H., Kearson, M. L., and Eraikhuemen, N. (2021). The impact of anticoagulation on covid-19 (sars cov-2) patient outcomes: a systematic review. *Journal of Pharmacy Practice*, page 08971900211015055.
- Lazo-Langner, A., Goss, G., Spaans, J., and Rodger, M. (2007). The effect of low-molecular-weight heparin on cancer survival. a systematic review and meta-analysis of randomized trials. *Journal of Thrombosis and Haemostasis*, 5(4):729–737.
- Leytin, V., Mody, M., Semple, J. W., Garvey, B., and Freedman, J. (2000). Flow cytometric parameters for characterizing platelet activation by measuring p-selectin (cd62) expression: theoretical consideration and evaluation in thrombin-treated platelet populations. *Biochemical and biophysical research communications*, 269(1):85–90.
- Michelson, A. D., Barnard, M. R., Krueger, L. A., Valeri, C. R., and Furman, M. I. (2001). Circulating monocyte-platelet aggregates are a more sensitive marker of in vivo platelet activation than platelet surface p-selectin: studies in baboons, human coronary intervention, and human acute myocardial infarction. *Circulation*, 104(13):1533–1537.
- Peerschke, E. I. and Zucker, M. B. (1981). Fibrinogen receptor exposure and aggregation of human blood platelets produced by adp and chilling. *Blood*, 57(4):663–670.
- Rampotas, A. and Pavord, S. (2021). Platelet aggregates, a marker of severe covid-19 disease. *Journal of Clinical Pathology*, 74(11):750–751.
- Ramstack, J., Zuckerman, L., and Mockros, L. (1979). Shear-induced activation of platelets. *Journal of biomechanics*, 12(2):113–125.
- Ren, S., He, K., Girshick, R., and Sun, J. (2015). Faster r-cnn: Towards real-time object detection with region proposal networks. *Advances in neural information processing systems*, 28.
- Riedl, J., Ay, C., and Pabinger, I. (2017). Platelets and hemophilia: A review of the literature. *Thrombosis research*, 155:131–139.
- Sibbing, D., Braun, S., Jawansky, S., Vogt, W., Mehilli, J., Schömig, A., Kastrati, A., and von Beckerath, N. (2008). Assessment of adp-induced platelet aggregation with light transmission aggregometry and multiple electrode platelet aggregometry before and after clopidogrel treatment. *Thrombosis and haemostasis*, 99(01):121–126.
- Suzuki, S. et al. (1985). Topological structural analysis of digitized binary images by border following. *Computer vision, graphics, and image processing*, 30(1):32–46.
- Ugele, M., Weniger, M., Stanzel, M., Bassler, M., Krause, S. W., Friedrich, O., Hayden, O., and Richter, L. (2018). Label-free high-throughput leukemia detection by holographic microscopy. *Advanced Science*, 5(12):1800761.
- Wallén, N. H., Ladjevardi, M., Albert, J., and Bröijersén, A. (1997). Influence of different anticoagulants on platelet aggregation in whole blood; a comparison between citrate, low molecular mass heparin and hirudin. *Thrombosis research*, 87(1):151–157.
- Whiting, D. and DiNardo, J. A. (2014). Teg and rotem: technology and clinical applications. *American journal of hematology*, 89(2):228–232.